



Title	STRUCTURAL PROPERTIES OF PHYCOERYTHRIN FROM DULSE PALMARIA PALMATA
Author(s)	Miyabe, Yoshikatsu; Furuta, Tomoe; Takeda, Tomoyuki; Kanno, Gaku; Shimizu, Takeshi; Tanaka, Yoshikazu; Gai, Zuoqi; Yasui, Hajime; Kishimura, Hideki
Citation	Journal of food biochemistry, 41(1), UNSP e12301 https://doi.org/10.1111/jfbc.12301
Issue Date	2017-02
Doc URL	http://hdl.handle.net/2115/68247
Rights	This is the peer reviewed version of the following article: UNSP e12301-Journal of food biochemistry, 2017-02, 41(1) UNSP e12301-, which has been published in final form at DOI: 10.1111/jfbc.12301. This article may be used for non-commercial purposes in accordance with Wiley Terms and Conditions for Self-Archiving.
Type	article (author version)
File Information	kishimura.pdf



[Instructions for use](#)

1 **STRUCTURAL PROPERTIES OF PHYCOERYTHRIN**
2 **FROM DULSE PALMARIA PALMATA**

3
4 **YOSHIKATSU MIYABE¹, TOMOE FURUTA¹, TOMOYUKI TAKEDA¹, GAKU**
5 **KANNO¹, TAKESHI SHIMIZU², YOSHIKAZU TANAKA^{3,4}, ZUOQI GAI³,**
6 **HAJIME YASUI⁵ and HIDEKI KISHIMURA^{6,7}**

7
8 ¹ Chair of Marine Chemical Resource Development, Graduate School of Fisheries Sciences,
9 Hokkaido University, Hakodate, Hokkaido 041-8611, Japan

10 ² Department of Research and Development, Hokkaido Industrial Technology Center,
11 Hakodate, Hokkaido 041-0801, Japan

12 ³ Laboratory of X-Ray Structural Biology, Faculty of Advanced Life Science, Hokkaido
13 University, Sapporo 060-0810, Japan

14 ⁴ Japan Science and Technology Agency, PRESTO, Sapporo 060-0810, Japan

15 ⁵ Laboratory of Humans and the Ocean, Faculty of Fisheries Sciences, Hokkaido University,
16 Hakodate, Hokkaido 041-8611, Japan

17 ⁶ Laboratory of Marine Chemical Resource Development, Faculty of Fisheries Sciences,
18 Hokkaido University, Hakodate, Hokkaido 041-8611, Japan

19

20 ⁷ Corresponding author.

21 TEL/FAX: 81-138-40-5519

22 EMAIL: kishi@fish.hokudai.ac.jp

23

24 **Short title:** Structural properties of dulse phycoerythrin

25

26 **ABSTRACT**

27 We found that the red alga dulse (*Palmaria palmata*) contains a lot of proteins, which is
28 mainly composed of phycoerythrin (PE), and the protein hydrolysates showed high
29 angiotensin I converting enzyme (ACE) inhibitory activities. Therefore, we investigated the
30 structure of dulse PE to discuss its structure-function relationship. We prepared the
31 chloroplast DNA and analyzed the nucleotide sequences encoding PE by cDNA cloning
32 method. It was clarified that dulse PE has α - and β -subunits and they are composed by 164
33 amino acids (MW: 17,638) and 177 amino acids (MW: 18,407), respectively. The dulse PE
34 contained conserved cysteine residues for chromophore attachment site. On the alignment
35 of amino acid sequences of dulse PE with those of other red algal PE, the sequence identities
36 were very high (81-92%). In addition, we purified and crystallized the dulse PE, and its
37 crystal structure was determined at 2.09 Å resolution by molecular replacement method.
38 The revealed 3-D structure of dulse PE which forms an ($\alpha\beta$)₂ hexamer was similar to other
39 red algal PEs. On the other hand, it was clarified that the dulse PE proteins are rich in
40 hydrophobic amino acid residues (51.0%), especially aromatic amino acid and proline
41 residues. The data imply that the high ACE inhibitory activity of dulse protein hydrolysates
42 would be caused by the specific amino acid composition and sequence of dulse PE.

43

44

45 **PRACTICAL APPLICATIONS**

46 Dulse is an abundant and underused resource, which contains a lot of phycobiliproteins.
47 Then, the dulse protein hydrolysates strongly inhibited the activity of angiotensin I converting
48 enzyme. Therefore, it has the potential to be an ingredient of functional food.

49

50

51 **KEYWORDS:** Red alga; Dulse; *Palmaria palmata*; ACE inhibitory activity; phycoerythrin;

52 Primary structure; 3-D structure

53

54 INTRODUCTION

55

56 In red algae, phycobiliproteins locate as phycobilisomes on the stromal side of thylakoid
57 membranes in a chloroplast and play a role of light capturing on photosynthesis (Apt *et al.*
58 1995; Sekar and Chandramohan 2008). The prominent classes of red algal phycobiliproteins
59 are phycoerythrin (PE) followed by phycocyanin (PC) and allophycocyanin (APC), and they
60 are divided on their spectral properties (λ -max of PE = 490-570 nm, λ -max of PC = 610-625
61 nm, λ -max of APC = 650-660 nm) (Sun *et al.* 2009). Phycobiliproteins of red algae
62 commonly contain α - and β -subunits, and each subunit bears covalently binding one or
63 several phycobilin chromophores at the specific cysteine residues (PE: phycoerythrobilin and
64 phycourobilin, PC: phycocyanobilin and phycoerythrobilin, APC: phycocyanobilin) (Apt *et al.*
65 1995). The above spectroscopic property of each phycobiliprotein is derived from the
66 specific chromophore composition. The α - and β -subunits of phycobiliprotein combine with
67 each other to form an ($\alpha\beta$) heterodimer, and then three ($\alpha\beta$)s form ($\alpha\beta$)₃ trimer arranging a
68 symmetry disc (Apt *et al.* 1995). The discs are organized in supramolecular complexes
69 called phycobilisomes. The core of phycobilisomes is composed of APC discs and the rod is
70 composed of PC and PE discs. On the previous proteomic and genomic studies, some
71 marine red algal phycobiliproteins were studied (Roell and Morse 1993; Ducret *et al.* 1994;
72 Hagopian *et al.* 2004; Niu *et al.* 2006; Tajima *et al.* 2012; Wang *et al.* 2013; DePriest *et al.*
73 2013). However, there is no information about structural properties of dulse
74 phycobiliproteins.

75 Dulse (*Palmaria palmata*) is a red alga mainly distributed in high-latitude coastal
76 areas, and it is popular in Ireland and Atlantic Canada as a food and a source of minerals.
77 Fitzgerald *et al.* (2012) and Harnedy *et al.* (2015) also reported the dulse protein hydrolysates
78 show the inhibitory effects for renin and dipeptidyl peptidase IV, respectively. In Japan,

79 dulse is also distributed around the coast of Hokkaido Prefecture and at Pacific coast of
80 Aomori Prefecture. However, dulse is rarely eaten in Japan. In addition, dulse is even
81 removed from Kombu (*Laminaria* sp.) farming areas in Hokkaido, because it inhibits the
82 growth of young Kombu in winter season. Therefore, we have begun exploring the health
83 benefits of dulse to advance its use as a functional food material. In the previous study, we
84 found that dulse contains a lot of proteins, which are mainly composed of PE followed by PC
85 and APC (Furuta *et al.*, 2016). Then, the dulse protein hydrolysates strongly inhibited the
86 activity of angiotensin I converting enzyme (ACE). Moreover, it was suggested that the
87 ACE inhibitory peptides are mainly derived from the dulse PE by thermolysin hydrolysis.
88 Therefore, in this study, we investigated the primary and 3-D structures of dulse PE to discuss
89 its structure-function relationship.

90 MATERIALS AND METHODS

91

92 Materials

93

94 Dulse (*P. palmata*) was collected in the coast of Usujiri, Hokkaido, Japan in February. A
95 portion of the thalli was steeped into RNAlater solution (Applied Biosystems, CA, USA) and
96 stored at -80 °C until use.

97 Restriction enzymes, *Hind* III and *Ssp* I, were purchased from TaKaRa Bio (Shiga,
98 Japan). RNase A was purchased from Nacalai Tesque (Kyoto, Japan). ACE from rabbit
99 lung was purchased from Sigma Chemical Co. (Mo, USA). Hyppuryl-L-histidyl-L-leucine
100 (Hip-His-Leu), thermolysin (EC 3.4.24.27) from *Bucillus thermoproteolyticus*, pepsin (EC
101 3.4.23.1) from porcine stomach, and trypsin (EC 3.4.21.4) from bovine pancreas were
102 purchased from Wako Pure Chemical (Osaka, Japan). All other reagents were purchased
103 from Wako Pure Chemical (Osaka, Japan).

104

105 Preparation of dulse protein hydrolysates

106

107 The frozen samples were lyophilized and ground into a fine powder by Wonder Blender
108 WB-1 (OSAKA CHEMICAL Co., Osaka, Japan). Proteins were extracted from the powder
109 by adding 20 v/w of distilled water at 4 °C for 7 h. The extracts were centrifuged (H-200,
110 Kokusan, Tokyo, Japan) at 4 °C, 15,000 x g for 10 min, and then the supernatants were used
111 as “dulse proteins”. Some of the dulse proteins were hydrolyzed by 1.0 wt% of thermolysin
112 at 70 °C for 3 h, and the reaction was terminated by heat treatment at 100 °C for 5 min.
113 Subsequently, the solution was centrifuged at 4 °C, 15,000 x g for 10 min. The supernatants
114 were dried by lyophilization into the “thermolysin hydrolysates”. Other dulse proteins were

115 adjusted to pH 2.0, and the proteins were digested by 1.0 wt% of pepsin at 37 °C for 3 h.
116 After the reaction, the pepsin digests were adjusted to pH 8.0. Subsequently, the solutions
117 were centrifuged at 4 °C, 15,000 x g for 10 min. The supernatants were dried by
118 lyophilization into the “pepsin hydrolysates”. Some of the pepsin hydrolysates were
119 digested by 1.0 wt% of trypsin at 37 °C for 3 h. After that, the digested solutions were
120 boiled for 5 min to inactivate the enzymes, and then centrifuged at 4 °C, 15,000 x g for 10 min.
121 The supernatants were dried by lyophilization into the “pepsin-trypsin hydrolysates”.

122

123 ACE Inhibitory Assay

124

125 ACE inhibitory assay was carried out according to the method of Cheung and Cushman
126 (1973) with some modifications. Fifteen microliters of sample solution (5.0 mg/mL) was
127 added to 30 μ L of 1.0 M sodium borate buffer (pH 8.3) and the mixture was

128 Thirty microliters of Hip-His-Leu solution (12.5 mM in 0.1 M sodium borate buffer
129 containing 400 mM NaCl at pH 8.3) was added to the mixture. After incubation at 37 °C for
130 1 h, the reaction was stopped by adding 75 μ L of 1.0 M

131 was extracted with 450 μ L of ethyl acetate. Four hundred microliters of the upper layer was
132 evaporated, and then the hippuric acid was dissolved in 1.5 mL of distilled water. The
133 absorbance at 228 nm of the solution was measured by a spectrophotometer. The inhibition
134 was calculated from the equation $[1 - (As - Asb) / (Ac - Acb)] \times 100$, where Ac is the absorbance
135 of the buffer, Acb is the absorbance when the stop solution was added to the buffer before the
136 reaction, As is the absorbance of the sample, and Asb is the absorbance when the stop solution
137 was added to the sample before the reaction.

138

139

140 Isolation of Dulse Chloroplast DNA

141

142 Thawed dulse sample was dissected with scissors and 150 mg of it was put into a
143 microcentrifuge tube. The sample was homogenized in 1.5 mL of TRIzol reagent
144 (Invitrogen, CA, USA) using disperser. Then, 300 μ L of chloroform was added to the
145 homogenate, and the solution was mixed. The mixture was centrifuged at 4 $^{\circ}$ C, 15,000 x g
146 for 20 min, and the supernatant was pooled in a micro tube. Next, equal volume of
147 2-propanol was added in the tube to precipitate chloroplast DNA, and the solution was
148 centrifuged at 4 $^{\circ}$ C, 15,000 x g for 20 min. The precipitate was dissolved in 100 μ L of TE
149 buffer, and the remaining RNA in it was removed by RNase A treatment (10 μ g, 37 $^{\circ}$ C, 30
150 min). After the reaction, 200 μ L of sterilized ultrapure water and 300 μ L of
151 phenol-chloroform-isoamyl alcohol (25:24:1, v/v/v) were added, and the mixed solution was
152 centrifuged at 4 $^{\circ}$ C, 15,000 x g for 15 min. Following similar treatment with
153 chloroform-isoamyl alcohol (24:1, v/v), chloroplast DNA was collected by ethanol
154 precipitation. The dried precipitate was dissolved in 100 μ L of TE buffer.

155

156 Degenerate PCR

157

158 Forward primer (PE-F1: ATGCT (A/C/G/T) AA (C/T) GC (A/C/G/T) TTTTC (A/C/G/T)
159 (A/C) G) and reverse primer (PE-R1: CC (A/C/G/T) GC (A/G/T) AT (A/C/G/T) CCCCCA
160 (C/T) TC (A/G) TC) for degenerate PCR were designed on the basis of well-conserved
161 regions of red algal PE genes (*rpeB* and *rpeA*) (Fig. 1a). TaKaRa EX *Taq* Hot Start Version
162 (TaKaRa Bio, Shiga, Japan) was used on the amplification. The PCR program for TaKaRa
163 EX *Taq* HS was 40 cycles of 98 $^{\circ}$ C for 10 sec, 47 $^{\circ}$ C for 30 sec, 72 $^{\circ}$ C for 2 min, and 10 min
164 at 72 $^{\circ}$ C. The PCR products were separated by low melting agarose gel electrophoresis and

165 were purified from the gel using Wizard SV Gel and PCR Clean-Up System (Promega, WI,
166 USA).

167

168 Inverse PCR

169

170 The remaining 5'- and 3'-regions of dulse PE genes were determined by inverse PCR method.

171 Dulse chloroplast DNA was digested with restriction enzymes, *Ssp* I and *Hind* III. The

172 digested DNA fragments were cleaned by Mini Elute Spin Columns (QIAGEN, Dusseldorf,

173 Germany), and ligated with T4 DNA ligase (TaKaRa Bio, Shiga, Japan) at 16 °C for 18 h.

174 For amplifications, specific forward (PE-IF1: CATTACTGATGGTAACAAACGC, PE-IF2:

175 GAGACGTTGATCATTATATGCG) and reverse (PE-IR1: TCACTGCCACCAACGTAAGC,

176 PE-IR2: CTCCACCTTCTTTTACAACAGC) primers were designed using the sequence data

177 determined by degenerate PCR (Fig. 1b). TaKaRa EX *Taq* Hot Start Version (TaKaRa Bio,

178 Shiga, Japan) was used on the amplification, and the PCR program was 40 cycles of 98 °C for

179 10 sec, 50 °C for 30 sec, 72 °C for 2 min, and 10 min at 72 °C.

180

181 Cloning and Sequencing

182

183 PCR products were subcloned to pDrive Cloning Vector using QIAGEN PCR Cloning Kit

184 (QIAGEN, Dusseldorf, Germany) for sequencing. The nucleotide sequences of cDNAs

185 were determined with BigDye Terminator v3.1 Cycle Sequencing Kit (Applied Biosystems,

186 CA, USA) using ABI PRISM 310 Genetic Analyzer (Applied Biosystems, CA, USA).

187 Nucleotide and deduced amino acid sequences of dulse PE gene were aligned using

188 CLUSTAL W program (Thompson, *et al.* 1994). Molecular weight and isoelectric point of

189 dulse PE were calculated from deduced amino acid sequences by using Compute pI/Mw tool

190 (Bjellqvist *et al.* 1993; Bjellqvist *et al.* 1994; Hoogland *et al.* 2000).

191

192 Crystallization, X-ray diffraction data collection, and structure determination

193

194 Frozen dulse samples (-30 °C) were taken into a flask, and 4 volumes (v/w) of distilled water
195 was added in it. The dulse phycobiliproteins were extracted at 4 °C for 12 h, and the extracts
196 were filtered. Then, the filtrates were centrifuged at 4 °C, 15,000 x g for 15 min. The
197 extracted dulse proteins were dialyzed against distilled water at 4 °C for 24 h. The dulse PE
198 was purified from the protein extracts by a preparative electrofocusing using Rotoform system
199 (Bio-Rad, CA, USA) (Fig. 4a and 4b). Crystallization was carried out by hanging-drop
200 vapor diffusion method. Crystals of dulse PE were grown from a buffer containing 0.1 M
201 sodium acetate (pH 4.8) and 12% PEG4000 (Fig. 4b). X-ray diffraction dataset of dulse PE
202 was collected on the beamline BL17A at Photon Factory (Tsukuba, Japan) under cryogenic
203 condition (100 K). Crystals were mounted on the X-ray diffractometer after soaked into a
204 crystallization buffer containing 20% PEG400 as a cryoprotectant. The diffraction data were
205 indexed, integrated, scaled, and merged using the XDS program (Kabsch 2010). The data
206 statistics are shown in Table 1. Crystal structures were determined by the molecular
207 replacement method with the program MOLREP (Vagin and Teplyakov 1997) using the
208 structure of PE from *Polysiphonia urceolata* (PDB ID 1LIA) as a search model. To monitor
209 the refinement, a random 5% subset was set aside for the calculation of the R_{free} factor.
210 Structure refinement was carried out with phenix.refine (Adams *et al.* 2010). The
211 stereochemical quality of the structure was analyzed with the program MOLPROBITY (Chen
212 *et al.* 2010). The refinement statistics are summarized in Table 1. The atomic coordinates
213 of dulse PE has been deposited in the Protein Data Bank, www.pdb.org (PDB ID code 5B13).

214 **RESULTS AND DISCUSSION**

215

216 Inhibition of ACE activity of dulse protein hydrolysates

217

218 In the previous study, we found that dulse contains a lot of proteins, which are mainly
219 composed of PE (Furuta *et al.* 2016). The extracted dulse proteins showed slight ACE
220 inhibitory activity, but the activity was extremely enhanced by thermolysin hydrolysis. In
221 addition, nine ACE inhibitory peptides (YRD, AGGEY, VYRT, VDHY, IKGHY, LKNPG,
222 LDY, LRY, FEQDWAS) were isolated from the hydrolysates by reversed-phase
223 high-performance liquid chromatography (HPLC), and the sequences of YRD, AGGEY,
224 VYRT, VDHY, LKNPG, LDY and LRY were detected in the primary structures of PE α - and
225 β -subunits (Furuta *et al.* 2016). From these results, it was suggested that the ACE inhibitory
226 peptides are mainly derived from the dulse PE by thermolysin hydrolysis. Therefore, in this
227 study, we prepared the dulse protein hydrolysates by thermolysin, pepsin, and pepsin-trypsin
228 digestion, and we compared with their ACE inhibitory activity. As shown in Fig. 2, the
229 thermolysin hydrolysates inhibited 88% of ACE activity, and pepsin and pepsin-trypsin
230 hydrolysates also suppressed 72% and 75% of them, respectively. We calculated the peptide
231 sequences derived from the deduced amino acid sequences of dulse PE α - and β - subunits by
232 using PEPTIDEMASS (Wilkins *et al.* 1997). As a result, it was predicted that 76 peptides
233 (α -subunit: 38 peptides, av. length=3, av. mass=346; β - subunit: 38 peptides, av. length=4, av.
234 mass=396) are derived from dulse PE α - and β - subunits by pepsin-trypsin hydrolysis. From
235 the result, ACE inhibitory peptides are also produced from dulse proteins, especially PE, by
236 proteolytic hydrolysis in our digestive tract. In future, we would like to analyze the
237 structural properties of ACE inhibitory peptides in the pepsin-trypsin hydrolysates to compare
238 with those of thermolysin hydrolysates.

239 Then, in the next stage, we investigated the primary and 3-D structures of dulse PE
240 to discuss its structure-function relationship.

241

242 Nucleotide sequences of dulse phycoerythrin genes

243

244 In this study, we obtained 1,560 bp of nucleotide sequences on the analysis of the dulse PE
245 gene, and the gene structure encoding dulse PE (*rpeA* and *rpeB*, GenBank accession number
246 AB625450) (Fig. 3) was clarified. This is the first report for the PE gene of Palmariales.

247 As shown in Fig. 3, the dulse PE gene was constituted of α - and β -subunit genes and
248 A/T-rich spacer. AT contents of the spacer in dulse PE gene were 79% (60 bp/76 bp).
249 Bernard *et al.* (1992) reported that *rpeB* gene of *Rhodella violacea* is split by intervening
250 sequence and the sequence has a feature of group II intron that is typical in eukaryotic
251 organisms, however the dulse PE gene has no introns. The dulse *rpeB* was present in prior
252 to the *rpeA* (Fig. 3). The positions of *rpeA* and *rpeB* were the same as those of other red
253 algae, for example *Gracilaria tenuistipitata* (Hagopian *et al.* 2004), *Chondrus crispus*
254 (GenBank accession number HF562234), *Pyropia yezoensis* (Wang *et al.* 2013), *P.*
255 *haitanensis* (Wang *et al.* 2013) and *P. purpurea* (GenBank accession number U38804). The
256 nucleotide sequences of dulse PE gene also showed considerably high identities (about 80%)
257 with those of other red algae (Table 2). The GC contents in dulse PE gene were about 40%
258 (*rpeA*: 40.2%, *rpeB*: 40.5%), and these numerical values showed very high similarity to those
259 of *P. yezoensis* (*rpeA*: 42.6%, *rpeB*: 40.6%), *P. haitanensis* (*rpeA*: 41.2%, *rpeB*: 41.4%) and *P.*
260 *purpurea* (*rpeA*: 41.8%, *rpeB*: 42.0%), whereas it was a little higher than those of *G.*
261 *tenuistipitata* (*rpeA*: 37.0%, *rpeB*: 38.8%) and *C. crispus* (*rpeA*: 37.2%, *rpeB*: 39.1%) (Table
262 2).

263 The consensus sequences at -10 (5'-TATAAT-3') and -35 (5'-TTGACA-3')

264 promoter elements for RNA polymerase were searched in the dulse PE genes. As a result,
265 putative motifs were found at upstream regions of *rpeB* (-10: TATATT or TGTAAT, -35:
266 TAAACA or GAAACA) (single and double underlines in Fig. 3). We also sought out the
267 Shine-Dalgarno sequence (5'-AGGAGGT-3') acting as a binding site with 16S rRNA, and
268 then the homologous structures were detected in the upstream of each gene (*rpeB*: AGGAGA,
269 *rpeA*: AGGAGA,) (dotted underlines in Fig. 2).

270

271 Primary structure of dulse phycoerythrin

272

273 The deduced amino acid sequences of dulse PE α - and β -subunits are shown in Fig. 3. The
274 PE α -subunit consists of 164 amino acids (495 bp), and its molecular weight and isoelectric
275 point were calculated at 17,638 and 5.40, respectively. Red algal PE commonly has two
276 kinds of chromophores, phycoerythrobilin and phycourobilin. Generally, red algal PE
277 α -subunit binds to two phycoerythrobilin with two Cys residues (Lundell *et al.* 1984; Ficner
278 *et al.* 1992), and the dulse PE α -subunit also retained Cys residues at the corresponding
279 positions (α Cys82 and α Cys139 in Fig. 3 and Fig. 4a). The dulse PE β -subunit consists of
280 177 amino acids (534 bp), and its molecular weight and isoelectric point were calculated at
281 18,407 and 5.42, respectively. It is already known that one phycourobilin and two
282 phycoerythrobilins bind to four Cys residues in β -subunit apo-protein through thioether
283 linkage (Lundell, *et al.* 1984; Ficner *et al.* 1992). In the dulse PE β -subunit, corresponding
284 Cys residues binding with phycourobilin (β Cys50 and β Cys61 in Fig. 3 and Fig. 4b) and with
285 phycoerythrobilins (β Cys82 and β Cys158) were all conserved.

286

287 3-D structures of dulse phycoerythrin

288

289 We purified and crystallized the dulce PE (Fig.5a), and its crystal structure was determined by
290 molecular replacement method (Fig.5b and Table 1). The revealed 3-D structure of purified
291 dulce PE in this study formed an ($\alpha\beta$)₆ hexamer, which was similar to other red algal PEs
292 (Chang *et al.* 1996; Contreras-Martel *et al.* 2001; Ritter *et al.* 1999). The root mean square
293 deviations (r.m.s.d) with other PEs are as follows, *Polysiphonia urceolata* PE: 0.70 Å,
294 *Griffithsia monilis* PE: 0.55 Å, *Gracilaria chilensis* PE: 0.60 Å. As observed for other
295 homologous phycobiliproteins such as PE, PC and APC, the backbone conformations of α -
296 and β -subunits of dulce PE have nine α -helices (X, Y, A, B, E, F', F, G, and H) as a dominant
297 secondary structure element (Fig. 5b) (Lundell *et al.* 1984; Ficner *et al.* 1992; Liu *et al.* 1999;
298 Jiang *et al.* 2001). Each subunit had a structure quite similar to those of other PEs. The
299 r.m.s.d. was 0.39 Å, 0.33 Å, and 0.37 Å for α -subunit, and 0.56 Å, 0.48Å, and 0.55Å for
300 β -subunit of *P. urceolata* PE, *G. monilis* PE and *G. chilensis* PE, respectively. The electron
301 density clearly showed the presence of chromophores covalently linked to Cys residue
302 through thioether bond. Phycoerythrobilins were linked covalently with each of α Cys82,
303 α Cys139, β Cys82, and β Cys158, whereas a phycourobilin was linked doubly to β Cys50 and
304 β Cys61. The presence of chromophores at these sites is highly conserved among PEs of
305 which structures have been reported (Camara-Artigas *et al.* 2012; Chang *et al.* 1996;
306 Contreras-Martel *et al.* 2001; Lundell *et al.* 1984; Ritter *et al.* 1999). Taken these
307 observations together, we concluded that dulce PE has structural characteristics common to
308 other PEs.

309

310 Structure-function relationship of dulce phycoerythrin

311

312 ACE is a key enzyme in the regulation of peripheral blood pressure catalyzing the production
313 of angiotensin II and the destruction of bradykinin (Cheung *et al.* 1980). The specific

314 inhibitors of the enzyme therefore have been considered with effective antihypertensive drugs.
315 In addition to the drugs, ACE inhibitory peptides from daily food are also useful for
316 maintaining blood pressure at a healthy level. Although the potency of peptide is lower than
317 drug, it does not have side effect (Balti *et al.* 2015). Up to now, many researchers have
318 identified various ACE inhibitory peptides from the enzymatic hydrolysates of food (Amado
319 *et al.* 2014; Ghassem *et al.* 2014; Balti *et al.* 2015; García-Moreno *et al.* 2015). Besides,
320 Cheung *et al.* (1980) obtained the interesting results by using several synthetic peptides for a
321 substrate of ACE, that is to say, the ACE inhibitory activity of peptide is closely related to the
322 C-terminal dipeptide residues in it. Specifically, in case of tryptophan, tyrosine, or proline
323 residue is located at the N-terminal side of dipeptide and aromatic amino acid or proline
324 residue is at the C-terminus, its inhibitory potency is the most. Indeed, it has been well
325 known that the peptides are usually composed of hydrophobic and aromatic amino acids
326 (Amado *et al.* 2014; Ghassem *et al.* 2014; Balti *et al.* 2015; García-Moreno *et al.* 2015).
327 Therefore, we calculated the contents of hydrophobic and aromatic amino acid residues in
328 dulse PE by using the primary structures in this study (Fig. 3). As a result, it was clarified
329 that the dulse PE are rich in hydrophobic amino acids (51.0%), especially the contents of
330 aromatic amino acids and proline (10.0-10.9%) are relatively high. On the other hand,
331 crystal structure analysis clearly showed that dulse PE shares significant similarity in their
332 tertiary structure with other PEs. Therefore, we concluded that the cause of high ACE
333 inhibitory activity of dulse PE hydrolysates would be the specific amino acid compositions
334 and sequences, independent of the tertiary structure.

335 **ACKNOWLEDGMENTS**

336

337 We thank Dr. Koji Mikami, Faculty of Fisheries Sciences, Hokkaido University, for the
338 technical assistance of inverse PCR. We thank Dr. Hiroki Saeki, Faculty of Fisheries
339 Sciences, Hokkaido University, for the technical assistance of preparative electrofocusing
340 using Rotofor system. We also thank Mr. Yuki Kato, Hokkaido Industrial Technology Center,
341 for the operative support of DNA sequencer.

342 This work was supported in part by the Regional Innovation Cluster Program
343 (Global Type), Ministry of Education, Culture, Sports, Science and Technology, Japan and the
344 Grant-in-Aid for High Technology Research Program from the Ministry of Education, Culture,
345 Sports, Science, and Technology of Japan. This work was supported in part by
346 Grants-in-Aid for Scientific Research (24000011, 20374225, and 16H00748 to YT) and
347 Platform for Drug Discovery, Informatics, and Structural Life Science from the Ministry of
348 Education, Culture, Sports, Science and Technology, Japan, and JST, PRESTO (YT).

349

350 **REFERENCES**

351

352 APT, K.E., COLLIER, J.L. and GROSSMAN, A.R. 1995. Evolution of the phycobiliproteins.
353 J. Mol. Biol. 248, 79-96.

354 ADAMS, P.D., AFONINE, P.V., BUNKOCZI, G., CHEN, V.B., DAVIS, I.W., ECHOLS, N.,
355 HEADD, J.J., HUNG, L.W., KAPRAL, G.J., GROSSE-KUNSTLEVE, R.W., MCCOY,
356 A.J., MORIARTY, N.W., OEFFNER, R., READ, R.J., RICHARDSON, D.C.,

357 RICHARDSON, J.S., TERWILLIGER, T.C. and ZWART, P.H. 2010. PHENIX:
358 a comprehensive Python-based system for macromolecular structuresolution.

359 Acta Crystallogr. D66, 213-221.

360 AMADO, I.R., VAZQUEZ, J.A., GONZALEZ, P., ESTEBAN-FERNANDEZ, D.,

361 CARRERA, M. and PINEIRO, C. 2014. Identification of the major ACE-inhibitory
362 peptides produced by enzymatic hydrolysis of a protein concentrate from cuttlefish
363 wastewater. Marine Drugs 12, 1390-1405.

364 BERNARD, C., THOMAS, J.C., MAZEL, D., MOUSSEAU, A., CASTETS, A.M., DE

365 MARSAC, N.T. and DUBACQ, J.P. 1992. Characterization of the genes encoding
366 phycoerythrin in the red alga *Rhodella violacea*: evidence for a splitting of the *rpeB* gene
367 by an intron. Proc. Natl. Acad. Sci. U.S.A. 89, 9564-9568.

368 BJELLQVIST, B., HUGHES, G., PASQUALI, C., PAQUET, N., RAVIER, F., SANCHEZ,

369 J.-C., FRUTIGER, S. and HOCHSTRASSER, D.F. 1993. The focusing positions of
370 polypeptides in immobilized pH gradients can be predicted from their amino acid
371 sequences. Electrophoresis 14, 1023–1031.

372 BJELLQVIST, B., BASSE, B., OLSEN, E. and CELIS, J.E. 1994. Reference points for

373 comparisons of two-dimensional maps of proteins from different human cell types defined
374 in a pH scale where isoelectric points correlate with polypeptide compositions.

375 Electrophoresis *15*, 529–539.

376 BALTI, R., BOUGATEF, A., SILA, A., GUILLOCHON, D., DHULSTER, P. and
377 NEDJAR-ARROUME, N. 2015. Nine novel angiotensin I-converting enzyme (ACE)
378 inhibitory peptides from cuttlefish (*Sepia officinalis*) muscle protein hydrolysates and
379 antihypertensive effect of the potent active peptide in spontaneously hypertensive rats.
380 Food Chem. *170*, 519-525.

381 CHEUNG, H.S. and CUSHMAN, D.W. 1973. Inhibition of homogeneous
382 angiotensin-converting enzyme of rabbit lung by synthetic venom peptides of *Bothrops*
383 *jararaca*. Biochim. Biophys. Acta *293*, 451-463.

384 CHEUNG, H.S., WANG, F.L., ONDETTI, M.A., SABO, E.F. and CUSHMAN, D.W. 1980.
385 Binding of peptide substrates and inhibitors of angiotensin-converting enzyme:
386 importance of the COOH-terminal dipeptide sequence. J. Biol. Chem. *25*, 401-407.

387 CHANG, W.R., JIANG, T., WAN, Z.L., ZHANG, J.P., YANG, Z.X. and LIANG, D.C. 1996.
388 Crystal structure of R-phycoerythrin from *Polysiphonia urceolata* at 2.8 Å resolution. J.
389 Mol. Biol. *262*, 721-31.

390 CONTRERAS-MARTEL, C., MARTINEZ-OYANEDEL, J., BUNSTER, M., LEGRAND, P.,
391 PIRAS, C., VERNEDE, X. and FONTECILLA-CAMPS, J.C. 2001. Crystallization and
392 2.2 Å resolution structure of R-phycoerythrin from *Gracilaria chilensis*: a case of perfect
393 hemihedral twinning. Acta Crystallogr. *D57*, 52-60.

394 CHEN, V.B., ARENDALL 3rd. W.B., HEADD, J.J., KEEDY, D.A., IMMORMINO, R.M.,
395 KAPRAL, G.J., MURRAY, L.W., RICHARDSON, J.S. and RICHARDSON, D.C. 2010.
396 MolProbity: all-atomstructure validation for macromolecular crystallography. Acta
397 Crystallogr. *D66*, 12-21.

398 CAMARA-ARTIGAS, A., BACARIZO, J., ANDUJAR-SANCHEZ, M.,
399 ORTIZ-SALMERON, E., MESA-VALLE, C., CUADRI, C., ... and ALLEN, J.P. 2012.
400 pH-dependent structural conformations of B-phycoerythrin from *Porphyridium cruentum*.
401 FEBS J. 279, 3680-91.

402 DUCRET, A., SIDLER, W., FRANK, G. and ZUBER, H. 1994. The complete amino acid
403 sequence of R-phycoyanin-I α and β subunits from the red alga *Porphyridium cruentum*:
404 structural and phylogenetic relationship of the phycocyanins within the phycobiliprotein
405 families. Eur. J. Biochem. 221, 563-580.

406 DEPRIEST, M.S., BHATTACHARYA, D. and LOPEZ-BAUTISTA, J.M. 2013. The plastid
407 genome of the red macroalga *Grateloupia taiwanensis* (Halymeniaceae). PLoS One, 8,
408 e68246.

409 FICNER, R., LOBECK, K., SCHMIDT, G. and HUBER, R. 1992. Isolation, crystallization,
410 structure analysis and refinement of B-phycoerythrin from the red alga *Porphyridium*
411 *sordidum* at 2.2 Å resolution. J. Mol. Biol. 228, 935-950.

412 FITZGERALD, C., MORA-SOLER, L., GALLAGHER, E., O'CONNOR, P., PRIETO, J.,
413 SOLER-VILA, A. and HAYES, M. 2012. Isolation and characterization of bioactive
414 pro-peptides with *in vitro* renin inhibitory activities from the macroalga *Palmaria*
415 *palmata*. J. Agric. Food Chem. 60, 7421-7427.

416 FURUTA, T., MIYABE, Y., YASUI, H., KINOSHITA, Y. and KISHIMURA, H. 2016.
417 Angiotensin I converting enzyme inhibitory peptides derived from phycobiliproteins of
418 dulce *Palmaria palmata*. Marine Drugs , 14, 32; doi:10.3390/md14020032.

419 GHASSEM, M., BABJI, A.S., SAID, M., MAHMOODANI, F. and AEIHARA, K. 2014.
420 Angiotensin I-converting enzyme inhibitory peptides from snakehead fish sarcoplasmic
421 protein hydrolysate. J. Food Biochem. 38, 140-149.

422 GARCIA-MORENO, P.J., ESPEJO-CARPIO, F.J., GUADIX, A. and GUADIX, E.M. 2015.
423 Production and identification of angiotensin I-converting enzyme (ACE) inhibitory
424 peptides from Mediterranean fish discards. *J. Func. Foods* 18, 95-105.

425 HOOGLAND, C., SANCHEZ, J.-C., TONELLA, L., BINZ, P.-A., BAIROCH, A.,
426 HOCHSTRASSER, D.F. and APPEL, R.D. 2000. The 1999 SWISS-2DPAGE database
427 update. *Nucleic Acids Res.* 28, 286–288.

428 HAGOPIAN, J.C., REIS, M., KITAJIMA, J.P., BHATTACHARYA, D. and DE OLIVEIRA,
429 M.C. 2004. Comparative analysis of the complete plastid genome sequence of the red alga
430 *Gracilaria tenuistipitata* var. *liui* provides insights into the evolution of rhodoplasts and
431 their relationship to other plastids. *J. Mol. Evol.* 59, 464-477.

432 HARNEDY, P.A., O'KEEFFE, M.B. and FITZGERALD, R.J. 2015. Purification and
433 identification of dipeptidyl peptidase (DPP) IV inhibitory peptides from the macroalga
434 *Palmaria palmata*. *Food Chem.* 172, 400-406.

435 JIANG, T., ZHANG, J.P., CHANG, W.R. and LIANG, D.C. 2001. Crystal structure of
436 R-phycoyanin and possible energy transfer pathway in the phycobilisomes. *Biophys. J.*
437 81, 1171-1179.

438 KABSCH, W. 2010. Xds. *Acta Crystallogr. D*66, 125-132.

439 LUNDELL, D.J., GLAZER, A.N, DELANGE, R.J. and BROWN, D.M. 1984. Bilin
440 attachment sites in the α - and β -subunits of B-phycoerythrin: amino acid sequence
441 studies. *J. Biol. Chem.* 259, 5472-5480.

442 LIU, J.Y., JIANG, T., ZHANG, J.P. and LIANG, D.C. 1999. Crystal structure of
443 allophycoyanin from red algae *Porphyra yezoensis* at 2.2- Å resolution. *J. Biol. Chem.*
444 274, 16945-16952.

445 NIU, J.F., WANG, G.C. and TSENG, C.K. 2006. Method for large-scale isolation and
446 purification of R-phycoerythrin from red alga *Polysiphonia urceolata* Grev. *Protein Expr.*

447 Purif. 49, 23-33.

448 ROELL, M.K. and MORSE, D.E. 1993. Organization, expression and nucleotide sequence of
449 the operon encoding R-phycoerythrin ~~Polysiphonia~~ units from the red
450 *boldii*. Plant Mol. Biol. 21, 47-58.

451 RITTER, S., HILLER, R. G., WRENCH, P. M., WELTE, W. and DIEDERICHS, K. 1999.
452 Crystal structure of a phycourobilin-containing phycoerythrin at 1.90- Å resolution. J.
453 Struc. Biol. 126, 86–97.

454 SEKAR, S. and CHANDRAMOHAN, M. 2008. Phycobiliproteins as a commodity: trends in
455 applied research, patents and commercialization. J. Appl. Phycol. 20, 113-136.

456 SUN, L., WANG, S., GONG, X., ZHAO, M., FU, X. and WANG, L. 2009. Isolation,
457 purification and characteristics of R-phycoerythrin from a marine macroalga
458 *Heterosiphonia japonica*. Protein Expr. Purif. 64, 146-154.

459 THOMPSON, J.D., HIGGINS, D.G. and GIBSON, T.J. 1994. CLUSTAL W: improving the
460 sensitivity of progressive multiple sequence alignment through sequence weighting,
461 positions-specific gap penalties and weight matrix choice. Nucleic Acids Res. 22, 4673-
462 4680.

463 TAJIMA, N., SATO, S., MARUYAMA, F., KUROKAWA, K., OHTA, H., TABATA, S.,
464 SEKINE, K., MORIYAMA, T. and SATO, N. 2012. Analysis of the complete chloroplast
465 genome of the unicellular red alga *Porphyridium purpureum*. Photosynthetic Res. 22,
466 156-159.

467 VAGIN, A. and TEPLYAKOV, A. 1997. MOLREP: an automated program for molecular
468 replacement. J. Appl. Crystallogr. 30, 1022-1025.

469 WILKINS M.R., LINDSKOG I., GASTEIGER E., BAIROCH A., SANCHEZ J.C.,
470 HOCHSTRASSER D.F. and APPEL R.D. 1997. Detailed peptide characterization using

471 PEPTIDEMASS - a World-Wide-Web-accessible tool. *Electrophoresis*, 18, 403-408.
472 WANG, L., MAO, Y.X., KONG, F.N., LI, G.Y., MA, F., ZHANG, B.L., SUN, P.P., BI,
473 G.Q., ZHANG, F.F., XUE, H.F. and CAO, M. 2013. Complete sequence and analysis of
474 plastid genomes of two economically important red algae: *Pyropia haitanensis* and
475 *Pyropia yezoensis*. *PLoS One*, 8, e65902.

476
477
478
479
480
481
482
483
484
485
486
487
488
489
490
491
492
493
494
495
496
497
498
499
500

(Captions to figures)

FIG. 1. GENERAL STRUCTURES OF RED ALGAL PHYCOERYTHRIN GENES AND POSITIONS OF PRIMERS USED IN DEGENERATE AND INVERSE PCRS.

- a: Positions of primers used in degenerate PCR.
- b: Positions of primers used in inverse PCR.

PE represent phycoerythrin. Sequences of each primer are shown in the text.
Restriction sites are expressed as *Ssp* I, *Hind* III.

FIG. 2. ACE INHIBITORY ACTIVITIES BY DULSE PROTEIN HYDROLYSATES.

- 1: ACE inhibitory activity with thermolysin hydrolysates.
- 2: ACE inhibitory activity with pepsin hydrolysates.
- 3: ACE inhibitory activity with pepsin-trypsin hydrolysates.

FIG. 3. NUCLEOTIDE AND DEDUCED AMINO ACID SEQUENCES OF DULSE PHYCOERYTHRIN GENE.

Asterisks show stop codon. Single and double underlines express putative -10 and -35 consensus sequences, respectively. Dotted underline is putative RNA polymerase-binding motif.

FIG. 4. ALIGNMENT OF AMINO ACID SEQUENCES OF RED ALGAL PHYCOERYTHRINS.

- a: PE α ; Phycoerythrin α -subunit.
- b: PE β ; Phycoerythrin β -subunit.

Asterisks show characteristic amino acid residues in the molecule. *P. palmata* (GenBank accession number: AB625450, in this study); *G. tenuistipitata* (AY673996), *C.*

501 *crispus* (HF562234), *P. yezoensis* (D89878), *P. haitanensis* (DQ449070), *P. purpurea* (U38804).

502

503 **FIG. 5.** DULSE PHYCOERYTHRIN CRYSTAL AND 3-D STRUCTURE OF DULSE

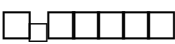
504 PHYCOERYTHRIN.

505 a: Crystallization of purified dulse phycoerythrin.

506 Purified PE: purified dulse phycoerythrin. PE crystal: dulse phycoerythrin crystal.

507 b: 3-D structure of dulse phycoerythrin.

508 PE ($\alpha\beta$  mer: Ribbon representation of dulse phycoerythrin

509 ($\alpha\beta$  mer) The α - and β -subunits are colored red and blue, respectively. For clarity,

510 one subunit of α - and β -subunit is colored orange and green, respectively. The bound CYC

511 and PUB are also shown as yellow and green sticks, respectively. PE α : Ribbon representation

512 of dulse phycoerythrin α -subunit. The model is colored according to the sequence from blue

513 at the N-terminus to red at the C-terminus. Bound CYC chromophores are shown as yellow

514 sticks. The cysteine residues linked with the chromophres are also shown. PE β : Ribbon

515 representation of dulse phycoerythrin β -subunit colored according to the sequence from blue

516 at the N-terminus to red at the C-terminus. Bound CYC and PUB chromophores are shown as

517 yellow and green sticks.

TABLE 1 DATA COLLECTION AND REFINEMENT STATISTICS

Data collection	
Beamline	Photon Factory BL17A
Space group	<i>C</i> 2
Cell dimensions	
a, b, c (Å)	187.5, 111.9, 112.7
α , β , γ (°)	90.0, 91.9, 90.0
Wavelength (Å)	0.98
Resolution (Å) ^a	50–2.09 (2.22–2.09)
No. of total/unique reflections	519,606/135,827 (81,130/21,390)
R_{sym} (%) ^{a, b}	11.6 (69.9)
Completeness (%) ^a	99.5 (97.6)
Multiplicity ^a	3.8 (3.8)
Average $I/\sigma(I)$ ^a	11.21 (2.13)
Refinement	
Resolution (Å)	50–2.09
$R_{\text{work}}/R_{\text{free}}$	0.198/0.237
No. of atoms	
Protein	15,114
Ligand	1,290
Solvent	1,812
r.m.s.d.	
Bond lengths (Å)	0.003
Bond angles (°)	1.318
Ramachandran plot	
Favored (%)	97.6
Allowed (%)	2.4
Outlier (%)	0

a Values in parentheses correspond to the highest resolution shell.

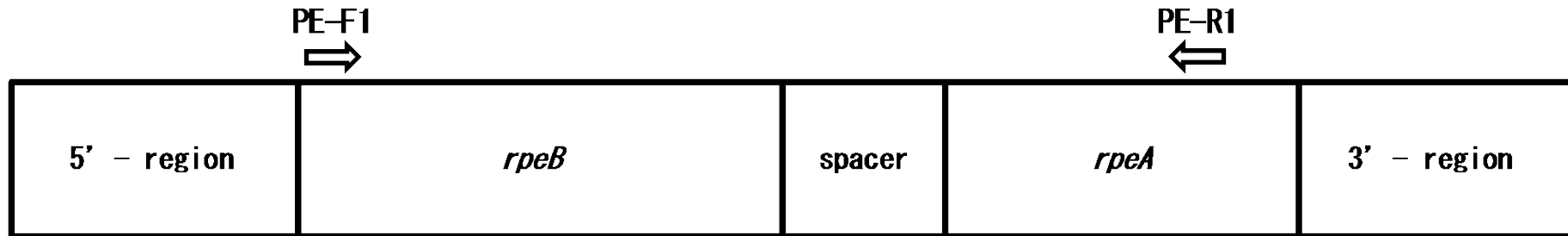
b $R_{\text{merge}} = \frac{\sum_h \sum_i |I_{h,i} - \langle I_h \rangle|}{\sum_h \sum_i |I_{h,i}|}$, where $\langle I_h \rangle$ is the mean intensity of a set of equivalent reflections.

TABLE 2. GC CONTENT, NUCLEOTIDE IDENTITY, AND AMINO ACID IDENTITY ON RED ALGAL PHYCOERYTHRINS

Organism	Gene name	GC content (%)	Nucleotide identity to <i>P.palmata</i> (%)	Amino acid identity to <i>P.palmata</i> (%)	Accession No.
<i>Palmaria palmata</i>	PE α -subunit	40.2	—	—	AB625450
	β -subunit	40.5	—	—	
<i>Gracilaria tenuistipitata</i>	PE α -subunit	37.0	79	87	AY673996
	β -subunit	38.8	78	81	
<i>Chondrus crispus</i>	PE α -subunit	37.2	82	85	HF562234
	β -subunit	39.1	80	85	
<i>Porphyra yezoensis</i>	PE α -subunit	42.6	82	89	D89878
	β -subunit	40.6	82	92	
<i>Porphyra haitanensis</i>	PE α -subunit	41.2	83	90	HM008261
	β -subunit	41.4	83	92	
<i>Porphyra purpurea</i>	PE α -subunit	41.8	82	90	NC_000925.1
	β -subunit	42.0	83	92	

FIG. 1

a: degenerate PCR



b: invers PCR

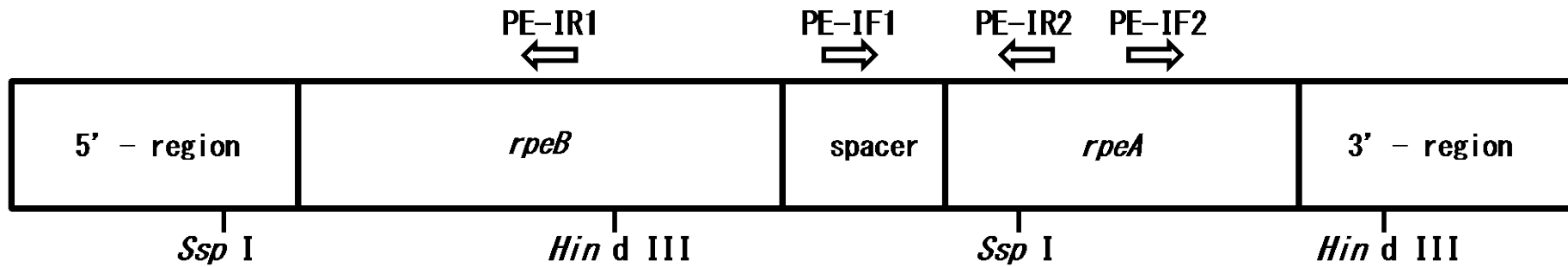


FIG. 2

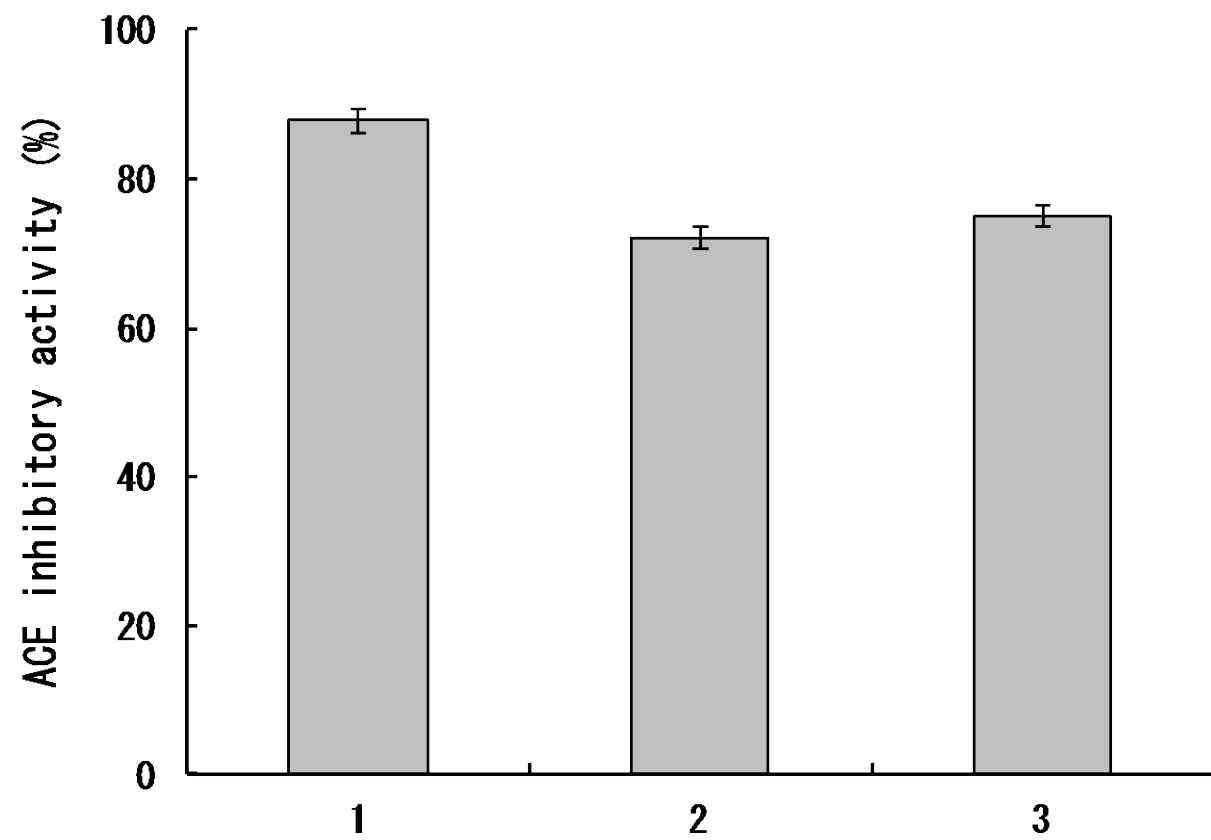


FIG. 3

5' -ATAATTAATTTATGATTA AAAACAGTAAGTTTTAAATCCTCTATTTTTAACTAAATTTTATTGTTACAATATATTACTTTGTTCTTAATAGGTTATTAGAAGTGCATATATTATGTAT 120
 TCGATACTAATACATCAGCAAGTTCAATTTTTAACAGCTGAAACAGCTAAGTCCTTTATATTTGTAATAAGGAGAGTTCATGCTTGACGCATTTTCCAGAGTTGTAGTAAATTCAGAC 240
 M L D A F S R V V V N S D
 GCTAAAGCTGCTTACGTTGGTGGCAGTGACCTACAGGCTCTAAAAAATTCATTACTGATGGTAACAAACGCTTAGATTCTGTTAGCTTTGTTGTTTCAAACGCTAGCTGTATCGTTTCT 360
 A K A A Y V G G S D L Q A L K K F I T D G N K R L D S V S F V V S N A S C I V S
 GATGCAGTATCAGGTATGATTTGTGAAAATCCTGGCTTAATTGCTCCTGGTGGTAATTGTTACACTAATCGTCGTATGGCTGCTGTCTACGTGATGGTGAAATCATTCTACGTTATGCT 480
 D A V S G M I C E N P G L I A P G G N C Y T N R R M A A C L R D G E I I L R Y A
 TCTTATGCTTTACTAGCTGGCGATCCTTCTGTACTAGAAGATCGTTGTCTTAATGGATTAAAAGAACTTACATTGCGTTAGGAGTTCCTACTAATTCATCAGTAAGAGCTGTAAGCATT 600
 S Y A L L A G D P S V L E D R C L N G L K E T Y I A L G V P T N S S V R A V S I
 ATGAAAGCTTCAGCTACAGCGTTTGTATCAGGCACAGCTTCTGACCGTAAAATGGCTTGTCCCTGATGGAGACTGTTGAGCTCTAGCATCAGAAGTAGGTAGCTATTGTGATAGAGTTGCT 720
 M K A S A T A F V S G T A S D R K M A C P D G D C S A L A S E L G S Y C D R V A
 GCTGCAATTAGCTAATAAAAGCTGTTATAGACTAGAGTATATAAATTTTTATACTCTTAGGCTAAATACTTAATAAAAAAAGGAGATTAATATGAAATCAGTTATGACTACAACGATTAG 840
 A A I S * M K S V M T T T I S
 TGCTGCAGACGCAGCTGGTGGTTTTCCCTTCATCTTCAGATCTTGAATCAGTTCAAGGTAATATTTCAACGTGCTGCTGCTAGATTAGAAGCTGCTGAAAAGTTAGCTAGTAATCATGAAGC 960
 A A D A A G R F P S S S D L E S V Q G N I Q R A A A R L E A A E K L A S N H E A
 TGTGTAAAAGAAGGTGGAGACGCTTGTGTTTCTAAGTATTCTTACTTAAAAATCCAGGTGAAGCTGGCGATAGCCAAGAAAAAGTAAACAAGTGTACAGAGACGTTGATCATTATAT 1,080
 V V K E G G D A C F A K Y S Y L K N P G E A G D S Q E K V N K C Y R D V D H Y M
 GCGTCTTGTAACCTATTCTTTAGTAGTTGGCGGAACTGGTCTCTTGTGAGTGGGCTATTGCTGGTCTCGTGAAGTTTATAGAAGTTTAAATCTTCCATCAGCTTCTTATGTTGCTGC 1,200
 R L V N Y S L V V G G T G P L D E W A I A G A R E V Y R T L N L P S A S Y V A A
 TTTGCTTTCACTCGTGATAGACTATGTGTGCCACGTGACATGTCTGCTCAAGCAGGTGGAGAATATGTTGCAGCTCTAGATTATATTGTTAATGCTTTAACCTAATTTATAGCTTGATA 1,320
 F A F T R D R L C V P R D M S A Q A G G E Y V A A L D Y I V N A L T *
 ATATAATAACAAATAAAATAGCTAAGCAAGCTTATTGCTTAGCTATTTTATTTGTTTATTGAACAATAAGCTCAGTTATGATATTGATGTATAGTACTATATAATATACGTAATT 1,440
 ATAAATACTACATACGTTGGAGCTTATTATGGATTCAAGTACAATGCAAAATACATGCATTAATATATCTTTTGGTCTTCTACTAGTGACTTTATTGGCTTATTGGACAAGTATTGCCTT- 3' 1,560

FIG. 4a

a: PE α

	1	10	20	30	40	50
<i>P. palmata</i>	M	KSV	MTT	TTT	ISA	AADA
<i>G. tenuistipitata</i>	M	KSV	ITT	V	ISA	AADA
<i>C. crispus</i>	M	KSV	ITT	I	ISA	AADA
<i>P. yezoensis</i>	M	KSV	ITT	T	T	T
<i>P. haitanensis</i>	M	KSV	ITT	T	T	T
<i>P. purpurea</i>	M	KSV	ITT	T	T	T
		**		*	*	*
	60	70	80	90	100	
<i>P. palmata</i>	V	VKE	G	D	A	C
<i>G. tenuistipitata</i>	V	VKE	A	G	D	A
<i>C. crispus</i>	V	VKE	A	G	D	A
<i>P. yezoensis</i>	V	VKE	A	G	D	A
<i>P. haitanensis</i>	V	VKE	A	G	D	A
<i>P. purpurea</i>	V	VKE	A	G	D	A
				*	*	
	110	120	130	140	150	
<i>P. palmata</i>	G	TG	P	L	D	E
<i>G. tenuistipitata</i>	G	TG	P	L	D	E
<i>C. crispus</i>	G	TG	P	F	D	E
<i>P. yezoensis</i>	G	TG	P	V	D	E
<i>P. haitanensis</i>	G	TG	P	V	D	E
<i>P. purpurea</i>	G	TG	P	V	D	E
		*		*		
	160					
<i>P. palmata</i>	E	Y	V	A	A	L
<i>G. tenuistipitata</i>	E	Y	T	T	A	L
<i>C. crispus</i>	E	Y	G	A	A	L
<i>P. yezoensis</i>	E	Y	A	G	N	L
<i>P. haitanensis</i>	E	Y	A	G	N	L
<i>P. purpurea</i>	E	Y	A	G	N	L

FIG. 4b

b: PE β

	1	10	20	30	40	50
<i>P. palmata</i>	MLDAFSRVVVNSDAKAAAYVGGSDLQALKKFI TDGNKRLDSVSFVVSNAS					
<i>G. tenuistipitata</i>	MLDAFSRVVIDSDTKAAAYVGGSNLQALKTFI SEGNQR L DAVNS I VSNASC					
<i>C. crispus</i>	MLDAFSRVVVNSDAKAAAYVGGSDLQALKTFI ADGNKRLDAVNS I VSNASC					
<i>P. yezoensis</i>	MLDAFSRVVVNSDAKAAAYVGGSDLQALKKFI ADGNKRLDSVNA I VSNASC					
<i>P. haitanensis</i>	MLDAFSRVVVNSDAKAAAYVGGSDLQALKKFI ADGNKRLDSVNA I VSNASC					
<i>P. purpurea</i>	MLDAFSRVVVNSDAKAAAYVGGSDLQALKKFI ADGNKRLDSVNA I VSNASC					
		*				*
		60	70	80	90	100
<i>P. palmata</i>	IVSDAVSGMI CENPGLI APGGNCYTNR RMAACLRDGE I ILRYASYALLAG					
<i>G. tenuistipitata</i>	IVSDAVSGMI CENPGLTSPGGNCYTNR RMAACLRDGE I ILRYISYALLAG					
<i>C. crispus</i>	IVSDAVSGMI CENPGLI APGGNCYTNR RMAACLRDGE I ILRYISYALLAG					
<i>P. yezoensis</i>	IVSDAVSGMI CENPGLI APGGNCYTNR RMAACLRDGE I ILRYVSYALLAG					
<i>P. haitanensis</i>	IVSDAVSGMI CENPGLI APGGNCYTNR RMAACLRDGE I ILRYVSYALLAG					
<i>P. purpurea</i>	IVSDAVSGMI CENPGLI APGGNCYTNR RMAACLRDGE I ILRYVSYALLAG					
		*	*	*	**	*
		110	120	130	140	150
<i>P. palmata</i>	DPSVLEDRCLNGLKETYIALGVPTNSSVR AVS IMKASATAFVSGTASDRK					
<i>G. tenuistipitata</i>	DPSVLEDRCLNGLKETYIALGVPTSSARAVN IMKASVAAFILNTAPGRK					
<i>C. crispus</i>	DASVLEDRCLNGLKETYIALGVPNSSIRS VV IMKAAAVAFVNNTASQRK					
<i>P. yezoensis</i>	DPSVLEDRCLNGLKETYIALGVPTNSSVR AVS IMKAAAVAFITNTASQRK					
<i>P. haitanensis</i>	DPSVLEDRCLNGLKETYIALGVPTNSSVR AVS IMKAAAVAFITNTASQRK					
<i>P. purpurea</i>	DPSVLEDRCLNGLKETYIALGVPTNSSVR AVS IMKASAVAFITNTASQRK					
		*				
		160	170			
<i>P. palmata</i>	MACPDGDCSALASELSYCDRVA A A I S					
<i>G. tenuistipitata</i>	MDTASGDCTALASEVGSYFDRVCA A I S					
<i>C. crispus</i>	MATTSGDCSALSAEVASYCDRVGA A L S					
<i>P. yezoensis</i>	MATADGDCSALASEVASYCDRVA A A I S					
<i>P. haitanensis</i>	MATADGDCSALASEVASYCDRVA A A I S					
<i>P. purpurea</i>	MATADGDCSALASEVASYCDRVA A A I S					
		*				

FIG. 5

a

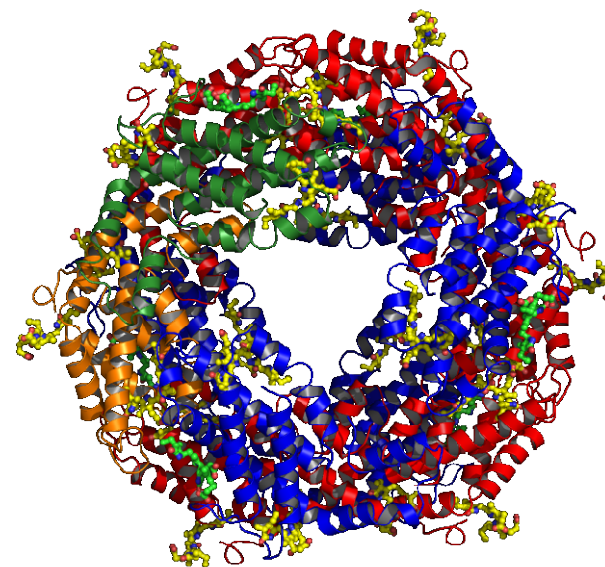


Purified PE

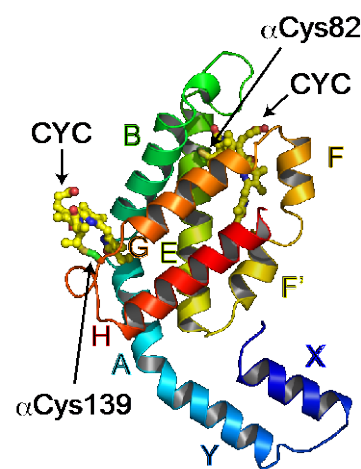


PE crystal

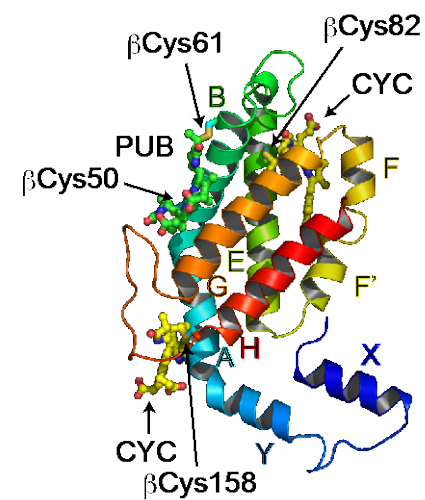
b



PE($\alpha\beta$)₆ hexamer



PE α



PE β